Centimeter- and Millimeter-Wave Channel Modeling Using Ray-Tracing for 5G Communications

Claude Oestges, Gauthier Hennaux and Quentin Gueuning
ICTEAM, Université catholique de Louvain
Louvain-la-Neuve, Belgium
Email: claude.oestges@uclouvain.be

***Abstract*—A ray-tracing tool, including specular reflection, diffraction and attenuation by foliage, is experimentally validated at 12 and 30 GHz in a suburban environment. The tool is then applied to double directional channel modeling at 30 GHz in a real-world urban area in downtown Brussels. Azimuth-, elevation- and delay-spread are computed and analyzed on a stochastic viewpoint. It is found that elevation spreads remain limited (below 3 degrees), while azimuth-spreads are on average similar at both sides of the link (with a mean value of 12 degrees). Delay-spreads vary significantly over the user's locations, with a mean value of 45 nanoseconds. They are positively correlated with the directional spreads at the base station. Finally, an investigation about the impact of microscopic surface roughness is conducted: it is found that it is mostly negligible at millimeter waves, unless extremely narrow beamwidth antennas are used.**

I. Introduction

UNDERSTANDING the radio channel behavior is essential to develop future millimeter-wave mobile systems as well as backhaul techniques, as recently proposed for 5G [1]. While attenuation by hydrometeors might not be a critical issue, centimeter- and millimeter-wave systems also encounter impairments from the local environment (buildings, trees and obstacles), especially in urban areas. While a number of recent experimental campaigns and ray-based simulation results were presented in [2], the number of experimental validations of electromagnetic modeling tools at millimeter wavelengths is still scarce [3]. Among numerical tools, ray-tracing approaches [4], [5] have gain significant interest in the last decade, mostly thanks to the progress in computation power. Ray-tracing offer the advantage to provide fast deterministic results, thereby replacing the need for costly measurements. However, ray-based models are not yet fully validated at centimetric and millimetric wavelengths.

In this paper, a ray-tracing tool accounting also for vegetation effects is compared with measurements recorded in the 12 and 30 GHz bands. Then, statistics of delay- and angle spreads are presented based on a large-scale simulation at 30 GHz. Finally, a few remarks about diffuse scattering are also discussed based on the implementation of rough surface scattering model.

This research was carried out within the research project B-WARE funded by WB-Health Program of the Walloon Region as well as within the European COST IC1004 Action.

II. Ray-Tracing Method at Higher Frequency Bands

The radio channel is modeled by means of a ray-tracing approach [5], accounting for the specular reflection by walls and ground, the diffraction by building wedges and the attenuation by trees. Diffuse scattering by trees and obstacles as well as transmissions through buildings are neglected in this paper. The reflected and diffracted fields are computed using the well known expressions based on the Fresnel theory and the Uniform Theory of Diffraction [6], in order to yield a fully polarimetric representation of the channel. The global channel, including the antennas at both link ends is then simply obtained by convolving each polarimetric path with the complex radiation patterns at both sides.

Each material (ground and building facade) is characterized by its complex relative electrical permittivity $\epsilon = \epsilon_r - j60\sigma\lambda$, where λ is the wavelength and ϵ_r and σ both depend on the frequency and material properties. Regarding vegetation, only the tree foliage is modeled in the simulations by means of parallelepipedic blocks representing the leaves. The foliage attenuation by single trees is modeled according to ITU-R P833-4 recommendation [7]. Scattering by foliage is not considered.

III. Experimental Validation

A. Measurement Setup

Experiments were carried out in a street of Louvain-la-Neuve in late summer and winter [8]. The street was lined on both sides by two-storey buildings as observed in Figure 1. In late summer, the link was obstructed by two deciduous trees in full foliage from the half of the experimental path. However, in the second measurement run, all branches had been cut off right before winter, so that trees were reduced to bare trunks.

The experimental transmit antennas, operating at 12.5 and 30 GHz (CW) were two corrugated circular horns with vertical polarization and a 3-dB beamwidth of 30 degrees. The receiver was a dual-band corrugated horn with vertical polarization and a 3-dB beamwidth of 20 degrees. It was kept fixed and placed on the roof of the highest (four-storey) building (Maxwell building) whereas the transmitter was successively moved away from the transmitter, stopping every meter to make a measurement, along a total distance of about 60 meters (at a

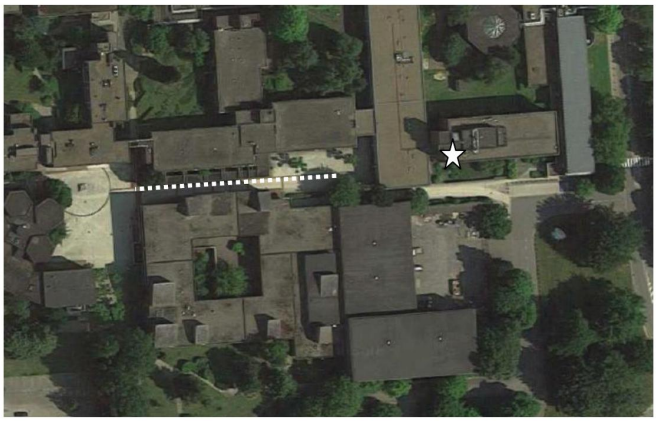

Fig. 1. Experimental environment (the star indicates the Tx location; the dashed line represents the Rx path)

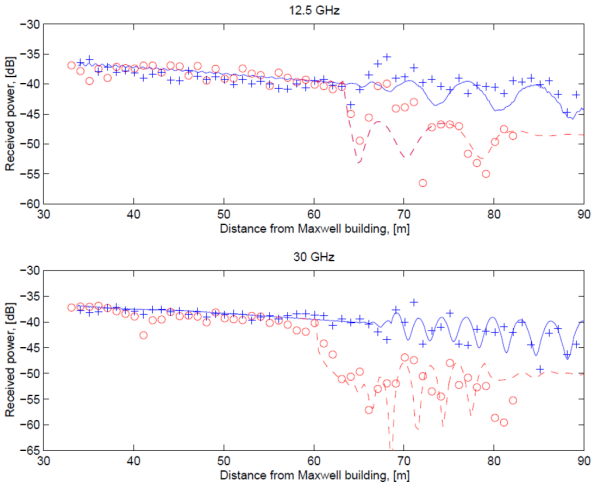

Fig. 3. Comparison between simulations and measurements at 12.5 GHz (upper graph) and 30 GHz (lower graph) : meas. February ('+') versus simulation without trees (solid lines), meas. October (circles) versus simulation including trees (dashed lines) [8]

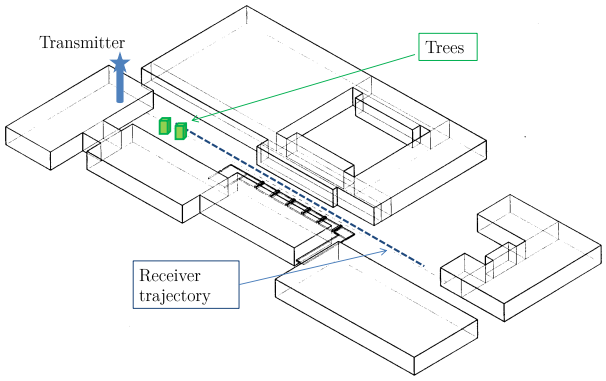

Fig. 2. Experimental environment (the star indicates the Tx location; the dashed line represents the Rx path), as simulated in the ray-tracing tool

height of 1.20 m). It is important to note that for each position of the mobile transmitter, the transmit antenna orientation was visually aligned along the boresight of the receiving antenna by means of an accurate 3D positioner.

B. Comparison with Ray-Tracing

To carry out the comparison, ground and building walls are assigned the following electromagnetic parameters (no tuning was performed): $\epsilon_r = 3.3$, $\sigma = 0$ S m-1 for walls at both frequencies, $\epsilon_r = 12$ and 5, $\sigma = 1.7$ S m-1 and 7.0 S m-1 for ground at 12.5 and 30 GHz respectively [9]. Figure 2 represents the simulated area, including the transmitter (Tx) and receiver (Rx) locations, as well as the considered trees.

Figure 3 shows the comparison between simulations and experimental results for all scenarios. For every test case, a good agreement can be observed on average. Since the received power was measured every meter, it is impossible for the experimental curves to reproduce each fading variation of the simulated signal. However, the fading statistics along the street are well reproduced, in particular the significant change taking place around 65 m. It is worth noting that is that only first-order reflections were accounted for in the simulations. Furthermore, the attenuation effect of foliage at both frequencies seems to be accounted for in a satisfactory fashion.

IV. Angle- and Delay Spread Statistics at 30 GHz

After validating the ray-tracing tool in the previous section, it has been applied to a typical urban area (roughly 300 m $\times$ 300 m) in Brussels, depicted in Figure 4. The ray-tracing used 3 reflections and single diffraction. Tree attenuation is neglected. The power received at the user equipment (UE) is normalized by assuming a unit transmit power. No antenna pattern is taken into account at this stage, i.e. antennas are assumed to be isotropic. This is obviously not realistic: however, millimeter-wave antenna patterns which will be used by 5G systems are not known at this stage. Furthermore, beamforming techniques require full directional information, so that the channel needs to be modeled independently of the antenna, as pointed out in [3]. The resulting radiomap is further depicted in Figure 5. At each UE location, the root-mean-square (RMS) angle- and delay-spreads are computed; their distributions are plotted in Figures 6 and refDS respectively.

We observe that the elevation spreads are limited: the mean elevation spreads are 1.6 and 3 degrees, respectively at BS and UE, ignoring the 14 % of locations for which the directional spreads are zero (meaning that only one ray was found at these locations). The azimuth spreads are similar, but highly variable at both BS and UE, reaching 11 degrees on average (with a standard deviation of 15 degrees).

The delay-spread remains limited, with an average value of 45 nanoseconds and a standard deviation of 50 nanoseconds.

Fig. 4. Simulated urban environment in Brussels (the star indicates the location of the base station (BS))

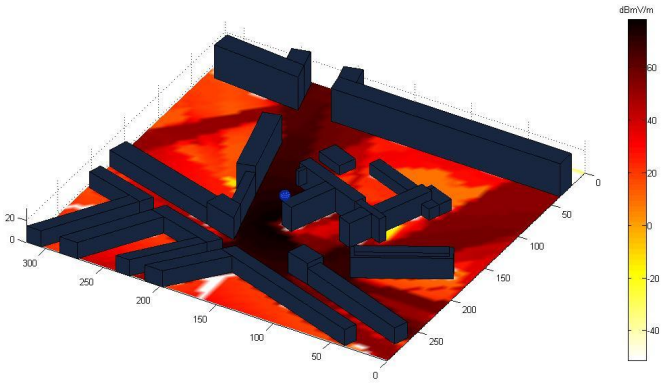

Fig. 5. Radiomap (average normalized field amplitude) at 30 GHz

Further calculations also reveal that it is positively correlated with direction spreads at BS (with correlation coefficients above 0.6), but no significantly correlated with the direction spreads at UE (with correlation coefficients below 0.2).

V. About Diffuse Scattering at 30 GHz

A. Diffuse Scattering Models

For a smooth surface, the reflected wave is coherent with the incident wave and is calculated by means of the reflection coefficient. If the surface gets slightly rough, this specular component is attenuated owing to scattering in all directions. That effect is accounted for by a reduction factor

$$\chi = \exp\left(-2k^2\Delta h_0^2 \cos^2\theta_i\right) \tag{1}$$

where k is the wavenumber, Δh_0 is the standard deviation of surface height and θ_i is the incidence angle. Hence, the

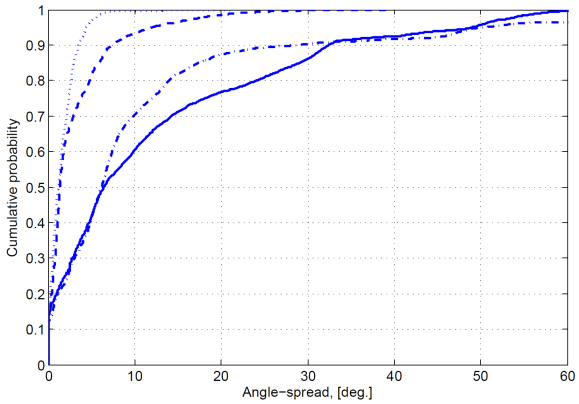

Fig. 6. Angular-spread cumulative distribution: elevation at UE (dashed), elevation at BS (dots) azimuth at UE (dot-dashed), azimuth at BS (solid)

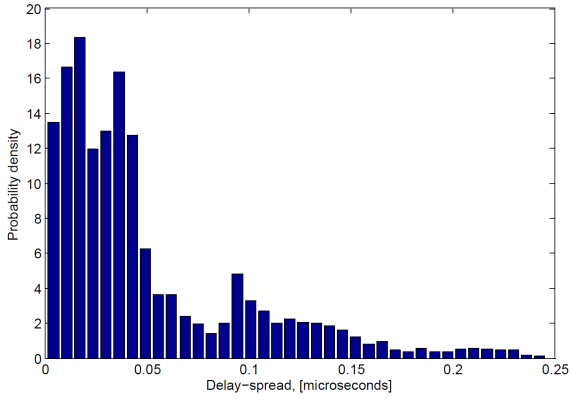

Fig. 7. Delay-spread distribution

specular reflected power can be expressed as:

$$P_{ref} = P_T \left(\frac{\lambda}{4\pi}\right)^2 \frac{G_T G_R}{(s+s')^2} R^2 \chi^2 \tag{2}$$

where

- P_T is the transmitted power,
- s is the path length between the transmitter and reflection point,
- s' is the path length between the reflection point and the receiver,
- R is the Fresnel reflection coefficient,
- G_T and G_R are the transmitter/receiver antenna gains.

Let us now consider an incident wave defined by a angle of incidence θ_i scattered by a surface whose roughness slope $\rho_0 = \Delta h_0/\Delta L_0$, ΔL_0 being the correlation length of surface height, defined as the distance for which the value of the correlation function of height variation decays by $1/e$. Individual bricks are typically characterized by a standard deviation of surface height Δh_0 of 0.1 mm [10], while for brick walls, average values from 1 mm to 5 mm and 6.2 mm are found in [11]–[13]. Finally, it seems reasonable to assume an order of magnitude of some centimeters for the correlation length

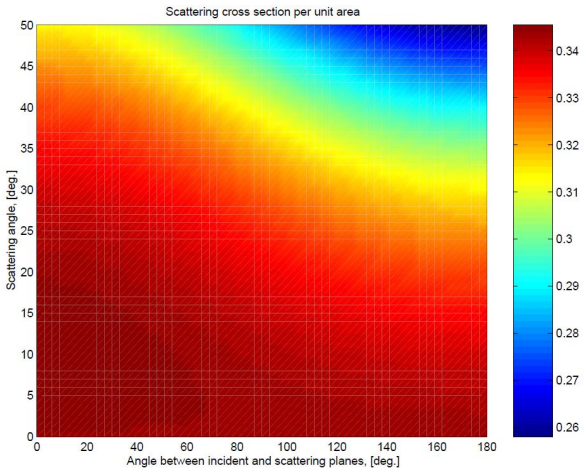

Fig. 8. Diffuse scattering cross section per unit area as a function of the scattering angle and the angle between incident and scattering planes

of usual brick walls. The diffuse power is scattered in all directions θ_s, with ϕ_s denoting the angle between the planes of incidence and scattering, and can be calculated [14] as

$$P_{sca} = P_T \left(\frac{\lambda}{4\pi}\right)^2 \int_S \frac{\sigma_{sca} G_T G_R}{4\pi r r'} ds \tag{3}$$

where r is the path length between transmitter and surface ds, r' is the path length between surface ds and receiver, and σ_{sca} is the scattering cross section per unit area of rough surface, which can be estimated using the Kirchhoff approximation. The latter is valid under the condition that the correlation length of the surface height L_0 is larger than the wavelength [10]. If the surface is very rough, i.e. when $|2\rho_0 (\cos\theta_i + \cos\theta_s)| > 1$, the Kirchhoff model for a Gaussian distributed surface height is outlined [14] by

$$\sigma_{sca} = \frac{\cos^2\theta_i}{(\cos\theta_i + \cos\theta_s)^2} \left[\frac{1 + \cos\theta_i \cos\theta_s - \sin\theta_i \sin\theta_s \cos\phi_s}{\rho_0 \cos\theta_i (\cos\theta_i + \cos\theta_s)}\right]^2 \cdot \exp\left[\frac{\sin^2\theta_i + \sin^2\theta_s - 2\sin\theta_i \sin\theta_s \cos\phi_s}{4\rho_0^2 (\cos\theta_i + \cos\theta_s)^2}\right] R^2 \tag{4}$$

For the following typical values: $\Delta h_0 = 6.2$ mm, $\Delta L_0 = 2$ cm, a roughness slope $\rho_0 = 0.3$ is obtained. At 30 GHz, this is not a very rough surface. However, the use of (4) can be considered as a first approximation.

Figure 8 depicts the scattering cross section per unit area of a wall ($\rho_0 = 0.3$) at 30 GHz as a function of the scattering angle and the angle ϕ_s. The incidence angle θ_i is assumed to be equal to 10 degrees. These values fulfill the validity condition of (4) for observation angles $\theta_s < 50$. In Figure 8, it is observed that the diffuse power is scattered in all directions, with no preference for the specular direction ($\phi_s = 0$, $\theta_s = \theta_i = 10$). Scattering is maximum in the direction perpendicular to the surface ($\theta_s = 0$) and decreases while both ϕ_s and θ_s increase.

Nevertheless, for such values of the scattering cross-section, rough surface scattering is not expected to play a significant role at 30 GHz. As an example, the diffuse power scattered by a typical plain brick wall of a few square meters will most likely be more than 30 dB below the LOS level. So, unless antennas are characterized by extremely narrow beamwidths and are used in strongly non-specular directions, diffuse scattering resulting from microscopic roughness should be negligible. At the same time, macroscopic diffuse scattering theories, such as those applied in [15] cannot really be used at such high frequency bands, as the characteristics dimensions of the roughness are much larger than the wavelength.

VI. Conclusion

A ray-tracing tool, including specular reflection, diffraction and attenuation by foliage, was successfully validated by measurements at 12 and 30 GHz in a suburban environment. Double directional channel selectivity was then analyzed at 30 GHz in a real-world urban area in downtown Brussels. It was observed that elevation spreads remain limited (below 3 degrees), while azimuth-spreads were on average similar at both sides of the link (with a mean value of 12 degrees). Delay-spreads might vary significantly over the user's locations, with a mean value of 45 nanoseconds and seemed to be positively correlated with the directional spreads at the base station. Finally, given the roughness of typical walls, it was shown that the diffuse component contribution might usually be neglected with respect to the specular one. There is one major exception at high frequencies (above X band): when the receiving antenna is characterized by a narrow beam, the specular component could be strongly attenuated if falling outside the beamwidth. For these cases, the diffuse contribution might become significant.

References

[1] T. Rappaport *et al.*, "Millimeter wave mobile communications for 5G cellular: it will work!" *IEEE Access*, no. 1, Jan. 2013.

[2] Y. Chang, S. Baek, S. Hur, Y. Mok, and Y. Lee, "A novel dual- slope mm-Wave channel model based on 3D ray-tracing in urban environments," in *Proc. IEEE Veh. Tech. Conf. Fall*, Sep. 2014.

[3] S. Hur, Y.-J. Cho, T. Kim, J. Park, A. Molisch, K. Haneda, and M. Peter, "mmWave spatial channel model in urban cellular environments at 28 GHz," in *Proc. European Conference on Antennas and Propagation (EuCAP)*, Lisbon, Portugal, 2015.

[4] A. Kanatas, I. Kountouris, G. Kostaras, and P. Constantinou, "A UTD propagation model in urban microcellular environments," *IEEE Trans. Veh. Tech.*, vol. 46, no. 1, pp. 185–193, Jan. 1997.

[5] F. Mani, "Improved ray-tracing for advanced radio propagation channel modeling," Ph.D. dissertation, Université catholique de Louvain, 2012.

[6] D. McNamara, C. Pistorius, and J. Malherbe, *Introduction to the Uniform Geometrical Theory of Diffraction*. Artech House, 1990.

[7] *ITU-R Recommendation P.833-4: Attenuation in vegetation*. ITU: Geneva, 2003.

[8] C. Oestges and D. Vanhonacker-Janvier, "Experimental validation and system applications of ray-tracing model in built-up areas," *Electronics Letters*, vol. 36, no. 5, p. 461462, mar. 2000.

[9] G. Van Dooren, "A deterministic approach to the modelling of electromagnetic wave propagation in urban environments," Ph.D. dissertation, Technische Universiteit Eindhoven, 1994.

[10] *COST 255: Radiowave propagation modelling for new SatCom services at Ku band and above*. European Commission: Brussels, 2001.

[11] F. Layer and H. Fruechting, "Modeling time-variant wideband indoor radio channels with rough scattering surfaces: a comparison," in *European Wireless '99*, Munich, Germany, Oct. 1999, pp. 279–284.

[12] O. Landron, M. Feuerstein, and T. Rappaport, "A comparison of theoretical and empirical reflection coefficients for typical exterior wall surfaces in a mobile radio environment," *IEEE Trans. Antennas Propagat.*, vol. 44, no. 3, pp. 341–351, March 1996.

[13] A. Hammoudeh, M. Sanchez, and E. Grindrod, "Experimental analysis of propagation at 62 GHz in suburban mobile radio microcells," *IEEE Trans. Veh. Tech.*, vol. 48, no. 2, pp. 576–587, Feb. 1999.

[14] A. Ishimaru, *Wave propagation and scattering in random media (vol. 2)*. Academic Press, 1978.

[15] V. Degli-Esposti, F. Fuschini, E. M. Vitucci, and G. Falciasecca, "Measurement and modelling of scattering from buildings," *IEEE Trans. Antennas Propagat.*, vol. 55, no. 1, pp. 143–154, Jan. 2007.